A genetic timer through noise-induced stabilization of an unstable state

Marc Turcotte*, Jordi Garcia-Ojalvo†, and Gürol M. Süel*‡§

*Department of Pharmacology, University of Texas Southwestern Medical Center, Dallas, TX 753903; †Departament de Física i Enginyeria Nuclear, Universitat Politècnica de Catalunya, Colom 11, E-08222 Terrassa, Spain; and ‡Green Center for Systems Biology, University of Texas Southwestern Medical Center, Dallas, TX 75390

Edited by José N. Onuchic, University of California at San Diego, La Jolla, CA, and approved August 27, 2008 (received for review July 1, 2008)

Stochastic fluctuations affect the dynamics of biological systems. Typically, such noise causes perturbations that can permit genetic circuits to escape stable states, triggering, for example, phenotypic switching. In contrast, studies have shown that noise can surprisingly also generate new states, which exist solely in the presence of fluctuations. In those instances noise is supplied externally to the dynamical system. Here, we present a mechanism in which noise intrinsic to a simple genetic circuit effectively stabilizes a deterministically unstable state. Furthermore, this noise-induced stabilization represents a unique mechanism for a genetic timer. Specifically, we analyzed the effect of noise intrinsic to a prototypical two-component gene-circuit architecture composed of interacting positive and negative feedback loops. Genetic circuits with this topology are common in biology and typically regulate cell cycles and circadian clocks. These systems can undergo a variety of bifurcations in response to parameter changes. Simulations show that near one such bifurcation, noise induces oscillations around an unstable spiral point and thus effectively stabilizes this unstable fixed point. Because of the periodicity of these oscillations, the lifetime of the noise-dependent stabilization exhibits a polymodal distribution with multiple, well defined, and regularly spaced peaks. Therefore, the noise-induced stabilization presented here constitutes a minimal mechanism for a genetic circuit to function as a timer that could be used in the engineering of synthetic circuits.

bifurcation | dynamics | circuit | stochastic | quantized cycle

Stochastic fluctuations in gene expression and protein concentrations are a natural by-product of biochemical reactions in cells. Properties of this biochemical noise within genetic circuits, such as their amplitude, distribution, and propagation, have been extensively characterized (1–9). Additionally, theoretical and experimental studies have established that such noise can induce stochastic switching between distinct and stable phenotypic states (5, 10–23). Noise within genetic circuits is therefore thought to contribute to phenotypic heterogeneity in genetically identical cellular populations. It has also recently been shown experimentally that noise can trigger cellular differentiation in fruit flies and bacteria (14, 17, 18, 24). Together, these studies establish that noise can play an active functional role in cellular processes by effectively destabilizing and thus inducing escape from stable phenotypic states.

Besides its common role in destabilizing stable states, noise can also have the more counterintuitive effect of generating new stable states that do not exist in the absence of fluctuations (25). In particular, noise-induced bistability has been reported theoretically (26, 27) and experimentally (2). In those situations, one of the two stable solution branches is usually present irrespective of fluctuations, whereas the second one is purely induced by noise (28). The appearance of such noise-induced branches of solutions requires particular nonlinearities in the underlying equations, and frequently an extrinsic noise source. It is thus of interest to establish mechanisms through which noise-induced stabilization can be caused by noise that is intrinsic to the biochemical reactions that comprise biological systems. Furthermore, because of the limited number of examples of noise-induced stabilization, it is unclear if and what different mechanisms can support this counterintuitive phenomenon.

The address the questions raised above, we have investigated a prototypical two-component activator–repressor genetic circuit as a model system (Fig. 1*A*). This circuit comprises a promoter (P_a) that expresses a transcription factor (A) that can activate both its own promoter (P_a) and the promoter of a repressor (P_r). The repressor protein (R) can inhibit the activity of the transcription factor (A) by targeting it for degradation. The autoregulation of the activator forms a positive feedback loop, whereas the activation of the repressor (R) and the consecutive inhibition of the activator molecule (A) by the repressor (R) establish a net negative feedback loop. Expression of activator and repressor transcription factors is thus synchronized where A and R can both be either high or low. Thus, this system constitutes a simple genetic circuit with interacting positive and negative feedback loops.

Natural genetic circuits that are composed of such interacting positive and negative feedback loops typically support various nonlinear dynamic behaviors (29). In particular, this circuit topology is common among genetic oscillators, such as cell cycle and circadian clocks (30–35). Additionally, transient cellular processes such as cell membrane polarization in neurons (36), yeast (37), and differentiation in bacteria (17, 18, 20) are also controlled by genetic circuits that are similar in architecture. Therefore, understanding how noise influences the dynamics of genetic circuits with this shared topology will be of general relevance to a wide range of cellular processes. Furthermore, a mechanistic understanding of the effects of noise on this simple circuit could guide the engineering of synthetic circuits with nonlinear dynamical behavior.

This investigation of the prototypical activator–inhibitor circuit described above shows that intrinsic noise is able to effectively stabilize an unstable state via a mechanism distinct and much simpler than those proposed to date. Below, we present results that demonstrate that intrinsic noise stabilizes an unstable fixed point that already exists deterministically. Specifically, when an unstable spiral point coexists with a second stable state from which it is separated by a saddle point, the phase-space topology is such that stochastic fluctuations are able to induce stochastic oscillations (38) around the unstable spiral. These oscillations in turn lead to increased dwell times in the region of space around the unstable fixed point, and therefore to its effective stabilization. We remark that, in our case, the effect is caused by standard intrinsic noise and does not require an external noise source.

Interestingly, this stabilization mechanism based on noise-induced oscillations around the unstable state also restricts the time window during which switching from the unstable high-expression

Author contributions: J.G.-O. and G.M.S. designed research; M.T. and J.G.-O. performed research; M.T., J.G.-O., and G.M.S. analyzed data; and J.G.-O. and G.M.S. wrote the paper.

The authors declare no conflict of interest.

This article is a PNAS Direct Submission.

Freely available online through the PNAS open access option.

§To whom correspondence should be addressed. E-mail: gurol.suel@utsouthwestern.edu.

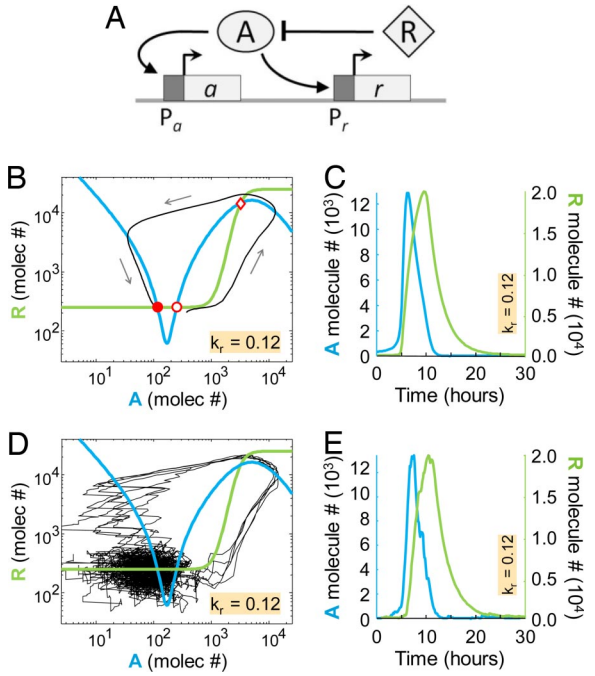

Fig. 1. Continuous and discrete stochastic simulations of a simple activator–repressor circuit generate qualitatively identical excitable dynamics. (*A*) Schematic diagram of the activator–repressor circuit. Activator and repressor proteins are denoted as A and R with corresponding genes *a*, *r* and promoters P_a and P_r, respectively. *B* and *D* as well as corresponding *C* and *E* compare continuous and discrete stochastic simulations of the repressor–activator circuit ($k_r = 0.12$). (*B*) Nullcline portrait of the activator–repressor circuit obtained from the two-dimensional continuous model described in the text. Activator and repressor nullclines are depicted in blue and green, respectively. One stable and two unstable fixed points at the three nullcline intersections are shown in filled red circle (stable node), open red circle (unstable saddle), and open red diamond (unstable focus), respectively. Black line denotes the continuous excitable trajectory of the system with gray arrows indicating its direction. (*C*) Continuous time traces of activator A (blue) and repressor R (green) molecule numbers during the transient excitable event shown in *B*. (*D*) The same nullcline portrait shown in *B* overlaid with five sample excitable trajectories (black) of excitable dynamics obtained from discrete stochastic simulations, which inherently account for biochemical noise within the repressor–activator circuit. Shown in *E* are stochastic time traces of activator *A* and repressor *R* molecule numbers during one of the excitable events shown in *D*.

state to the stable low-expression state can take place. Consequently, the unstable state is quasi-stable only for multiples of fixed duration, and the corresponding distribution of stabilization lifetimes is polymodal. Such polymodality has been reported in mammalian (39), yeast (40), and amphibian (41) cell cycles. Several mechanisms have been proposed to account for this polymodality, including specific gene circuits with complex dynamics (42, 43) and intercell communication (44). Our results hint at a simpler mechanism for such quantized cellular transitions. Furthermore, discretization of duration times for which the unstable state is stabilized represents a minimal mechanism for a genetic timer that could be used in synthetic biology.

Results

Comparing Continuous and Discrete Stochastic Simulations of Excitable Dynamics. To investigate the effect of noise on the dynamics of the activator–repressor circuit described above, we implemented a stochastic description in terms of a set of biochemical reactions compatible with the circuit architecture (Fig. 1*A*). From those reactions, one can derive a corresponding set of coupled ordinary differential equations that describe the dynamics of the activator and repressor:

$$\begin{aligned}\frac{da}{dt} &= k_1 + \frac{k_2 A^n}{K_a^n + A^n} - k_8 a \\ \frac{dr}{dt} &= k_3 + \frac{k_4 A^p}{K_r^p + A^p} - k_9 r \\ \frac{dA}{dt} &= k_5 a - k_7 A R - k_{10} A \\ \frac{dR}{dt} &= k_6 r - k_{11} R\end{aligned} \qquad [1]$$

These equations can be derived from the microscopic reactions underlying the circuit, listed in *Materials and Methods*. Here, A and R represent the concentration of activator and repressor proteins, respectively, a and r are the concentration of their corresponding mRNA molecules, and k_i are reaction rates (see *Materials and Methods* for definitions). Positive self-regulation of the activator A is represented by a Hill function with cooperativity exponent n and strength k_2, with half-maximal activation arising at a concentration of A equal to K_a. Similarly, A is also assumed to activate transcription of R following Hill kinetics with corresponding parameters p, k_4, and K_r.

Assuming that the dynamics of the mRNA molecules is much faster than that of the proteins (which is a reasonable assumption given that mRNA lifetimes are usually in the range of minutes, whereas protein lifetimes are in the range of hours, assuming no enzymatic degradation), we can adiabatically eliminate the equations for a and b, which leads to the following two-dimensional deterministic model:

$$\begin{aligned}\frac{dA}{dt} &= \alpha_a + \frac{\beta_a A^n}{k_a^n + A^n} - \delta A R - \lambda_a A \\ \frac{dR}{dt} &= \alpha_r + \frac{\beta_r A^p}{k_r^p + A^p} - \lambda_r R\end{aligned} \qquad [2]$$

The interpretation of the different terms occurring in these equations is as follows. Both species are assumed to be expressed at a basal rate given by α_a and α_r, and to degrade (for instance, because of growth dilution) at constant rates λ_a and λ_r, respectively. Regulated expression of A and R is controlled by the Hill functions with strengths β_a and β_r and rescaled Michaelis constants k_a and k_r, respectively (see *Materials and Methods*). Finally, repression of A by R is represented by the third term in the right-hand side of the A equation, and is controlled by the parameter δ. These parameters are related with the reaction rates of the differential equations (**1**) as follows:

$$\alpha_a = \frac{k_1 k_5}{k_8}, \quad \beta_a = \frac{k_2 k_5}{k_8}, \quad \alpha_r = \frac{k_3 k_6}{k_9}, \quad \beta_r = \frac{k_4 k_6}{k_9}$$
$$\delta = k_7, \quad \lambda_a = k_{10}, \quad \lambda_r = k_{11} \qquad [3]$$

By using the deterministic model **2**, we investigated the regime of excitable dynamics, in which threshold-crossing perturbations trigger well defined excursions in phase space. This regime occupies a broad region of parameter space, including parameter values typical for transcription, translation, and degradation processes. A representative set of such values is given in *Materials and Methods*. Nullcline analysis of the system showed that the excitable regime has three fixed points, two of which are unstable (Fig. 1*B*). Perturbations permit the system to escape the stable state (filled red circle in Fig. 1*B*) and undergo a well defined excursion around the unstable fixed points (open red symbols in the figure) and return to the stable fixed point, generating transient pulses of high activity for both activator and repressor molecules (Fig. 1*C*).

We then investigated the effect of biochemical noise on the behavior of the system by using discrete stochastic simulations of the

underlying biochemical reactions (see *Materials and Methods*), whose rates are related with the deterministic parameters of model **2** by means of the relations (Eq. **3**). For the resulting rates, the dynamics of the reactions were simulated by means of Gillespie's first reaction method (45). The stochastic phase-space trajectories shown in Fig. 1 *D* and *E* are similar to their deterministic counterparts and agree with the nullcline portrait corresponding to the deterministic model. Both deterministic and stochastic simulations generated transient pulses of high concentrations of activator and repressor during an excitable episode. Thus, accounting for biochemical noise within the genetic circuit in discrete stochastic simulations does not appear to introduce qualitatively different excitable dynamics when compared with continuous simulations.

Effect of Noise on Activator–Repressor Circuit Dynamics near a Bifurcation. Next we investigated how circuit dynamics behave when parameter values change, leading, in particular, to a bifurcation where the system transitions from one dynamical regime to another. Recent work showed that bifurcations from excitable to other dynamical regimes, such as oscillatory or bistability, are possible for a bacterial cellular differentiation circuit and yeast mating MAP kinase pathway *in vivo* (18, 46). Similarly, for the model system described in this study, changes in various parameter values can induce bifurcations. Specifically, here we investigated the dynamics of the activator–repressor system on changes in the binding affinity of the P_r promoter for the activator A, which is accounted for by the parameter k_r. Although the lower fixed point remains stable and the middle fixed point is unstable for all values of k_r studied, the upper fixed point undergoes a Hopf bifurcation and transitions from an unstable fixed point to a stable focus in response to increasing k_r values (Fig. 2*A*). This transition leads to a bistable regime for large k_r in which both the low- and high-concentration states for A and R molecules are stable.

What effect does noise have on the bifurcation scenario described above? To address this question, we compared continuous and discrete stochastic simulations for a value of k_r smaller than, but close to, the critical value beyond which the upper fixed point is stable. In the deterministic case, the unstable upper fixed point of the excitable regime is stabilized exactly at the Hopf bifurcation point. Before the bifurcation the genetic circuit continues to behave deterministically as an excitable system (Fig. 2 *B* and *C*). For the identical (smaller than critical) value of k_r, however, results from discrete stochastic simulations differ qualitatively, showing that the system can orbit around the unstable upper fixed point (Fig. 2*D*). During these oscillations concentrations of A and R molecules remain relatively high and near the unstable fixed point (Fig. 2*E*). Thus, noise within the genetic circuit appears to effectively stabilize the deterministically unstable upper fixed point, keeping the system in the high-expression state for prolonged periods of time.

Effective Stabilization of an Unstable Fixed Point by Noise. To establish the mechanism through which noise keeps the system in the high-expression state, we now turn to the phase-space analysis of model **2**. As mentioned above, the resting state of the system in the excitable regime corresponds to the stable fixed point indicated by the filled red circle at the bottom left of Fig. 3*A*. Of the two unstable fixed points, the upper one is an unstable focus (Fig. 3*A*, open red diamond), from which trajectories escape by spiraling outward. The middle fixed point is a saddle point (Fig. 3*A*, open red circle), from which four invariant trajectories emerge, two of them repulsive (data not shown in the figure), and two others attractive (Fig. 3*A*, magenta lines). The attractive invariant trajectories form the *stable manifold* of the saddle.

The part of the stable manifold that lies below the saddle is the excitability threshold, and separates deterministic trajectories corresponding to perturbations that lead to an excitable event from those leading to a direct (nonexcitable) relaxation to the stable fixed point. The part of the stable manifold above the saddle originates

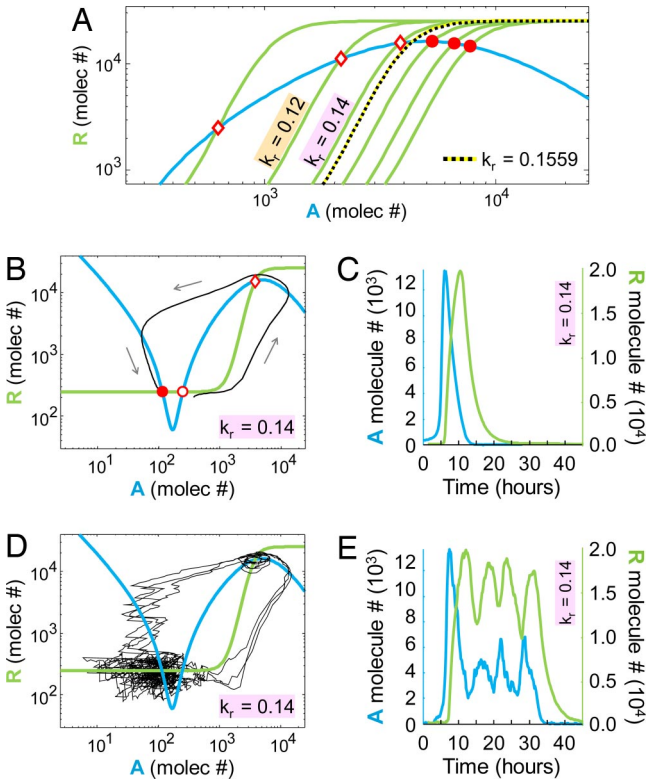

Fig. 2. Near a bifurcation, noise induces qualitative differences in activator–repressor circuit dynamics. (*A*) Enlarged view around the upper fixed point (in red) shown in Fig. 1 *B* and *D*, of activator and repressor nullclines in blue and green, respectively. For increasing values of the k_r parameter (which accounts for the binding affinity of the repressor promoter for activator protein), the blue activator nullcline shifts from left to right. At the critical value of $k_r = 0.1559$ (indicated with black-yellow dotted line) the upper fixed point undergoes a Hopf bifurcation and switches from an unstable focus (open red diamond) to a stable focus (filled red circle). Thus, for k_r values smaller than the critical value, the activator–repressor circuit constitutes an excitable system, whereas for higher k_r values the system is bistable. (*B* and *D*) Shown in black are excitable trajectories of continuous and discrete stochastic simulations, respectively, for a value of $k_r = 0.14$ for which the upper fixed point is deterministically unstable. Note that in *D*, the three sample trajectories obtained from discrete stochastic simulations orbit the upper deterministically unstable fixed point, whereas no such behavior is observed in the continuous simulation shown in *B*. (*C*) Continuous simulation time traces of activator and repressor molecule numbers are consistent with excitable dynamics as shown in Fig. 1*C*. (*E*) Discrete stochastic simulation time traces exhibit small oscillations at high molecule numbers that clearly differ from continuous simulation results shown in *C* obtained for identical k_r values.

from the unstable focus, from which it spirals outward, as shown in detail in Fig. 3*B*. This situation occurs typically when an unstable focus is located close to a saddle, for instance, right after a homoclinic bifurcation (47). The spiraling manifold line separates deterministic trajectories that lead directly to the stable fixed point (Fig. 3*B*, dashed black line) from those that are forced to orbit around the unstable focus before returning to the stable fixed point (Fig. 3*B*, solid black line). Trajectories can cross the manifold line many times resulting in consecutive orbits as shown in Fig. 2*E*. Such trajectories with more than one oscillation have their amplitude first reduced and then slowly increased until exit. This is because the oscillations spiral away from the unstable fixed point, whereas they cross the manifold line multiple times. In any case, as a result of such orbits, the time the trajectory spends near the unstable focus is increased, which can be viewed as an effective stabilization of the unstable focus.

Discretized Switching Between High and Low States of the Activator–Repressor Circuit due to Noise. Next, we investigated how the particular noise-induced mechanism described above affects the

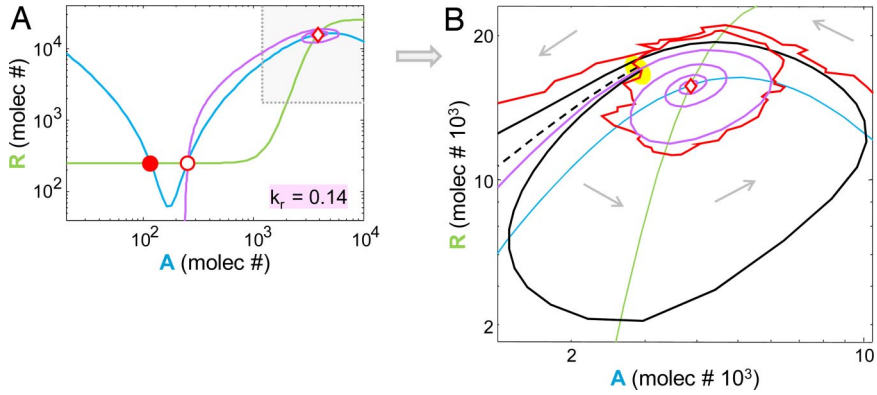

Fig. 3. Noise effectively stabilizes a deterministically unstable fixed point. (*A*) Phase portrait of the system for $k_r = 0.14$, with activator and repressor nullclines shown in blue and green, respectively. The deterministic stable manifold of the saddle point (open red circle) is shown in magenta. The stable fixed point is shown as a filled red circle, and the unstable focus as an open red diamond. (*B*) Enlarged view of phase portrait for the region around the upper unstable fixed point, as indicated by gray dotted line in *A*. Black lines are two deterministic trajectories with two different starting points with respect to the stable manifold (yellow-highlighted region). One of these trajectories (dashed black line) starts just outside of the stable manifold and returns directly to the stable fixed point shown in *A*. The other trajectory (solid back line) starts just inside the stable manifold and orbits the unstable fixed point once before returning to the stable fixed point. The red line is a trajectory obtained from discrete stochastic simulations. Noise inherent to the stochastic simulations causes the trajectory to cross the stable manifold (yellow-highlighted region). This results in the system orbiting the unstable fixed point at least once before ultimately returning back to the lower stable fixed point. This extends the time the system spends in the high-activity state and thus the duration of the trajectory.

nonlinear dynamic of the activator–repressor circuit. In the absence of noise, excitable events always take the system above the stable manifold, and thus never elicit oscillations around the unstable focus (Fig. 3*B*, dashed black line). In the presence of noise, however, stochastic fluctuations can force the trajectory to cross the stable manifold leading to tight orbits around the unstable focus, as shown by the red solid line in Fig. 3*B* (yellow-highlighted region in the figure). Such crossings might happen multiple times during the period the trajectory attempts to escape the unstable focus, leading to consecutive oscillations around the unstable focus. These orbits have a characteristic period, resulting in a quantized increase in the duration of the excitable event.

Interestingly, the noise-induced oscillations around the deterministically unstable focus lead to a quantization of the return times to the lower stable fixed point (Fig. 4*A*). The number of oscillations around the spiral point is given by the number of inward crossings of the manifold line minus the number of outward crossings (Fig. 3*B*). Because these oscillations have the same period, the return time is a multiple of this period. This quantization causes the genetic circuit to act as a timer, permitting the system to leave the high-expression state only at multiples of defined time periods (Fig. 4*A*). This effect results in a polymodal distribution of duration times, as shown in Fig. 4*B* for 5,000 excitable events at a fixed value of k_r relatively close to, but smaller than, the critical bifurcation value. Fig. 4*C* shows how the polymodal distribution emerges gradually as the value of k_r approaches the bifurcation, although it already exists well before that point. Thus, for a range of k_r values, noise inherent to the activator–repressor circuit induces the system to function as a genetic timer.

Discussion

Noise within genetic circuits is typically known to destabilize stable states (48, 49). Numerous studies have demonstrated that noise can provide the perturbation for a system to escape the attraction of stable states and trigger switching between distinct phenotypes (48, 50, 51). For example, the phage-λ lysis-lysogeny cellular decision-making switch was one of the first systems for which noise was proposed to be the trigger (52). More recent work has shown both theoretically and experimentally that noise initiates differentiation of *Bacillus subtilis* cells into competence (14, 17, 18, 20). The duration of proviral latency in HIV-1 has been suggested to be determined by noise in Tat, a transcription factor (53). Furthermore, noise-induced variability in gene expression between cells has been shown to generate phenotypic heterogeneity in genetically identical populations of cells (1, 7, 49, 51, 54). Other effects of noise include its ability to enhance oscillations in circadian clocks (29).

Despite the diverse organisms and model systems investigated, a common theme in the studies listed above is that noise provides the means to escape the attraction of a stable state. In this work,

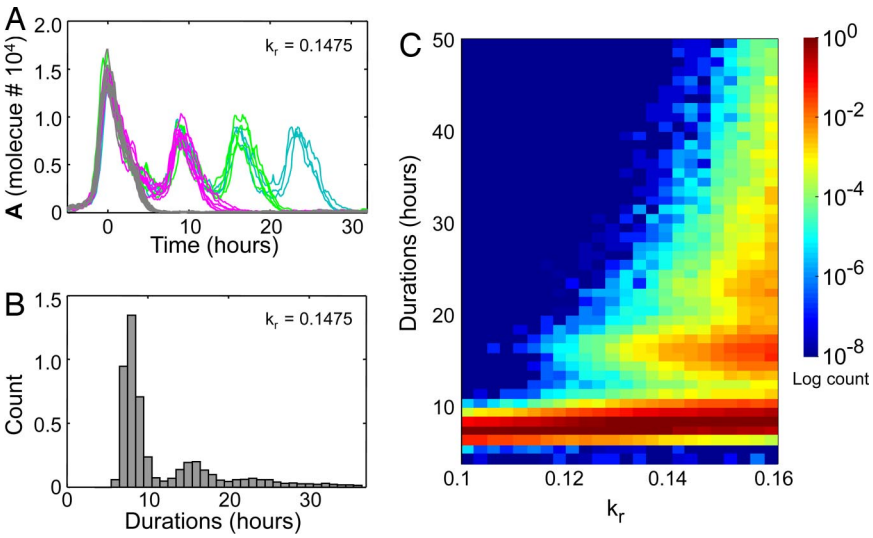

Fig. 4. Noise-induced stabilization generates quantized durations of activator–repressor circuit dynamics. *A* and *B* show results from discrete stochastic simulations obtained for $k_r = 0.1475$, which is smaller than the deterministically critical bifurcation value. (*A*) Sample time traces aligned in time with respect to maximum of first high molecule number peak. Depicted in gray, magenta, green, and blue are sample traces that orbit the deterministically unstable fixed point once, twice, three, or four times, respectively. Transitions from high- to low-molecule-number states are restricted to discretized time windows. (*B*) Histogram of duration times in high-activity state obtained from 5,000 trajectories including sample traces depicted in *A*. Note the polymodal nature of the distribution. (*C*) Histograms of high-activity-state durations (as shown in *B*) for indicated k_r values, normalized to its maximum for each k_r value, and color-coded with respect to the histogram of count values (in logarithmic scale). Note the polymodal distribution of duration times.

however, we present the opposite situation, in which stochastic fluctuations provide the means for a dynamical system to remain near an unstable state over time. Previous studies have addressed this issue by showing that noise is able to induce transitions leading to new states that do not exist in the absence of fluctuations (25). Hasty *et al.* (26), for instance, showed theoretically that noise-induced bistability can be used to design switches and amplifiers for gene expression. In another theoretical study, simulations of a prototypical enzymatic futile cycle suggested that noise can induce a behavior that differs qualitatively from what is predicted or possible deterministically (27). An experimental observation of noise-induced bistability was also reported by Blake *et al.* (2). In those studies, the origin of noise is external to the system, and thus, the specific coupling of this external noise to the system is critical. Here, we show, however, that in a simple two-component gene regulatory circuit, stochastic fluctuations inherent to the biochemical reactions that comprise the activator–repressor circuit can generate qualitatively distinct and deterministically inaccessible dynamics. Therefore, we demonstrated that external sources of noise are not necessary and that noise intrinsic to the genetic circuit can also induce dynamic behaviors. Furthermore, the dynamics observed in the activator–repressor circuit described here are unique in that they combine properties of excitable dynamics and bistability. The well defined durations of transient activity that are inherent to excitable dynamics are merged with the bistable property of switching between two distinct states, even though only one deterministically stable state exists. This fusion of excitability and bistability generate a dynamic behavior that combines switch-like behavior with periodicity.

The effect of noise on the dynamics of the simple activator–repressor circuit observed near a bifurcation also suggests possible evolutionary advantages. Simulations show that before bifurcation, noise allows the activator–repressor system to sample a dynamic regime that is deterministically accessible only after bifurcation. Therefore, noise appears to smear out the deterministically well defined bifurcation line into a region or area. This could have several biologically relevant advantages such as providing the system with the ability to sense distance to a critical bifurcation. Rather than an instant change in dynamics observed deterministically, the stochastic system undergoes a smooth transition from one dynamic regime to the next. In the region close to the bifurcation, the system can additionally exhibit a dynamic behavior that is a combination of the two dynamic regimes separated by the bifurcation. Furthermore, noise also expands the range of parameter values for which the activator–repressor circuit retains the ability to remain excitable, making excitability more robust against parameter changes. This work thus shows that noise within a genetic circuit can generate qualitatively different and dynamically unique behaviors that are accessible near bifurcations.

The stabilization of the unstable state of the activator–repressor circuit near the bifurcation interestingly occurs in a periodic manner. This mechanism allows the system to operate as a digital timer that controls transitions between the low and high gene expression states of the genetic circuit. Therefore, subpopulations of cells can switch from specific states with well defined wait times producing phenotypic heterogeneity within the population (Fig. 4*A*). Additionally, the mechanism described here generates a unique type of dynamic variability in the system. Rather than accessing the high gene expression state for random periods of time, as is common for bistable systems, here, the high-expression state is stabilized for well defined durations. This causes the system to behave as a genetic timer with a characteristic frequency.

This mechanism of noise-induced stabilization may be used in biological systems, in which exit from a certain cellular state needs to be correlated with periodic cellular activities such as the cell cycle or other metabolic rhythms without feedback control. For example, phenotypic switching and cellular differentiation requires the expression of hundreds of genes. To efficiently execute such cellular processes, it may be desirable to couple to metabolic cycles the probability of switching between states. Numerous examples of genetic circuits that share the simple architecture discussed here have been shown to regulate various processes in biological system (30–33, 55–58). It will thus be interesting to investigate whether the simple mechanism of a noise-induced timer presented here is used in the regulation of these cellular processes. Furthermore, polymodal distributions of cell cycle duration times have been reported in Chinese hamster V79 cells (39), in fission yeast (40), and during the early development of *Xenopus* embryos (41, 59). Because the topology of these eukaryotic cell cycle circuits is similar to that of the model described here, the observed quantized increases in cell cycle duration times may be explained by the proposed noise-induced stabilization phenomenon. In particular, the Anaphase Promoting Complex (APC) in eukaryotic cell cycles corresponds to the repressor molecule (R) in our model system. In combination with intrinsic noise, variations in the overall strength of the APC-mediated cell cycle negative feedback loop (corresponding to k_r in our model) could therefore give rise to the reported polymodal distribution of cell cycle times.

The simplicity of the two-component genetic circuit makes the noise-induced stabilization mechanism described here particularly accessible for synthetic biology applications. The noise-induced counter can be used to regulate the timing of phenotypic switching. Furthermore, no feedback control is necessary to couple phenotypic transitions to, for example, the cell cycle. Once the genetic circuit is triggered it can use its internal periodicity to exit at appropriate phases of the cell cycle. The minimal topology of the circuit is also ideal to experimentally tune the cycles of the counter. Therefore, this simple mechanism could be used to engineer synthetic circuits whose activities can be tuned and coupled to cyclic processes in the cell without requiring feedback control.

Materials and Methods

A set of reactions that respond to the architecture of the activator–inhibitor circuit shown in Fig. 1*A* is:

$$\mathrm{P}_A^{\mathrm{const}} \xrightarrow{k_1} \mathrm{P}_A^{\mathrm{const}} + \mathrm{mRNA}_A$$

$$\mathrm{P}_A \xrightarrow{f(A,k_2,K_a,n)} \mathrm{P}_A + \mathrm{mRNA}_A$$

$$\mathrm{P}_R^{\mathrm{const}} \xrightarrow{k_3} \mathrm{P}_R^{\mathrm{const}} + \mathrm{mRNA}_R$$

$$\mathrm{P}_R \xrightarrow{g(A,k_4,K_r,p)} \mathrm{P}_R + \mathrm{mRNA}_R$$

$$\mathrm{mRNA}_A \xrightarrow{k_5} \mathrm{mRNA}_A + \mathrm{A}$$

$$\mathrm{mRNA}_R \xrightarrow{k_6} \mathrm{mRNA}_R + \mathrm{R}$$

$$\mathrm{R} + \mathrm{A} \xrightarrow{k_7/\Omega} \mathrm{R}$$

$$\mathrm{mRNA}_A \xrightarrow{k_8} \varnothing$$

$$\text{mRNA}_R \xrightarrow{k_9} \varnothing$$

$$\text{A} \xrightarrow{k_{10}} \varnothing$$

$$\text{R} \xrightarrow{k_{11}} \varnothing$$

where P_A^{const} and P_A represent the constitutive and regulated promoters of the activator gene, respectively, with similar definitions for the repressor. The relation between concentrations and molecule numbers is given by the following factor:

$$\Omega = VA = 1.66\mu\text{m}^3 \times 6.023{\cdot}10^{23}\text{molec/mol} = 1 \text{ molec/nM}$$

where A is Avogadro's number, and V is the cell volume, which we assume here to have a value of 1.66 μm^3.

The rates of regulated transcription of the activator and repressor are given by the Hill functions:

$$f(A, k_2, K_a, n) = \frac{k_2 A^n}{K_a^n + A^n}, \qquad g(A, k_4, K_r, p) = \frac{k_4 A^p}{K_r^p + A^P}$$

where the Michaelis constants K_a and K_r are the half-maximal activation and repression molecule numbers, respectively. A set of parameters of the deterministic model **2** that leads to excitable dynamics is:

$$\alpha_a = 0.00875\ \text{s}^{-1}, \quad \beta_a = 7.5\ \text{s}^{-1}, \quad k_a = 0.2, \quad \lambda_a = 10^{-4}\ \text{s}^{-1}$$
$$\alpha_r = 0.025\ \text{s}^{-1}, \quad \beta_r = 2.5\ \text{s}^{-1}, \quad k_r = 0.12, \quad \lambda_r = 10^{-4}\ \text{s}^{-1}$$
$$\delta = 4.10^{-8}\ \text{molec}^{-1}, \quad n = 2, \quad p = 5$$

The Michaelis constants are $K_a = k_a\Gamma$ and $K_r = k_r\Gamma$, where $\Gamma = 2.5{\cdot}10^4$ molecules is a scaling factor. Now, assuming reasonable values for the rates of mRNA translation and degradation, $k_5 = k_6 = 0.2\ \text{s}^{-1}$ and $k_8 = k_9 = 0.005\ \text{s}^{-1}$, and using the relations given in Eq. **3**, one finds the following values for the rates of the remaining reactions:

$$k_1 = 0.00022\ \text{s}^{-1}, \quad k_2 = 0.1875\ \text{s}^{-1},$$
$$k_3 = 0.000625\ \text{s}^{-1}, \quad k_4 = 0.0625\ \text{s}^{-1}$$
$$k_7 = 4.10^{-8}\ \text{molec}^{-1}, \quad k^{10} = 10^{-4}\ \text{s}^{-1}, \quad k_{11} = 10^{-4}\ \text{s}^{-1}$$

ACKNOWLEDGMENTS. This work was supported by Spanish Ministry of Education and Science Project FIS2006-11452 and I3 program (J.G.O.) and the James S. McDonnell Foundation and the Welch Foundation (G.M.S.). M.T. is supported by National Institutes of Health Grant K25 GM071957. G.M.S. is a W.W. Caruth Jr. Scholar in Biomedical Research.

1. Bar-Even A, *et al.* (2006) Noise in protein expression scales with natural protein abundance. *Nat Genet* 38(6):636–643.
2. Blake WJ, *et al.* (2003) Noise in eukaryotic gene expression. *Nature* 422(6932):633–637.
3. Elowitz MB, *et al.* (2002) Stochastic gene expression in a single cell. *Science* 297(5584):1183–1186.
4. Newman JR, *et al.* (2006) Single-cell proteomic analysis of S. cerevisiae reveals the architecture of biological noise. *Nature* 441(7095):840–846.
5. Ozbudak EM, *et al.* (2002) Regulation of noise in the expression of a single gene. *Nat Genet* 31(1):69–73.
6. Pedraza JM, van Oudenaarden A (2005) Noise propagation in gene networks. *Science* 307(5717):1965–1969.
7. Raser JM, O'Shea EK (2004) Control of stochasticity in eukaryotic gene expression. *Science* 304(5678):1811–1814.
8. Swain PS, Elowitz MB, Siggia ED (2002) Intrinsic and extrinsic contributions to stochasticity in gene expression. *Proc Natl Acad Sci USA* 99(20):12795–12800.
9. Thattai M, van Oudenaarden A (2001) Intrinsic noise in gene regulatory networks. *Proc Natl Acad Sci USA* 98(15):8614–8619.
10. Ackers GK, Johnson AD, Shea MA (1982) Quantitative model for gene regulation by lambda phage repressor. *Proc Natl Acad Sci USA* 79(4):1129–1133.
11. Balaban NQ, *et al.* (2004) Bacterial persistence as a phenotypic switch. *Science* 305(5690):1622–1625.
12. Colman-Lerner A, *et al.* (2005) Regulated cell-to-cell variation in a cell-fate decision system. *Nature* 437(7059):699–706.
13. Ferrell JE Jr, Machleder EM (1998) The biochemical basis of an all-or-none cell fate switch in Xenopus oocytes. *Science* 280(5365):895–898.
14. Maamar H, Raj A, Dubnau D (2007) Noise in gene expression determines cell fate in Bacillus subtilis. *Science* 317(5837):526–529.
15. McAdams HH, Arkin A (1997) Stochastic mechanisms in gene expression. *Proc Natl Acad Sci USA* 94(3):814–819.
16. Novick A, Weiner M (1957) Enzyme induction as an all-or-none phenomenon. *Proc Natl Acad Sci USA* 43:553–566.
17. Suel GM, *et al.* (2006) An excitable gene regulatory circuit induces transient cellular differentiation. *Nature* 440(7083):545–550.
18. Suel GM, *et al.* (2007) Tunability and noise dependence in differentiation dynamics. *Science* 315(5819):1716–1719.
19. Thattai M, van Oudenaarden A (2004) Stochastic gene expression in fluctuating environments. *Genetics* 167(1):523–530.
20. Schultz D, *et al.* (2007) Molecular level stochastic model for competence cycles in Bacillus subtilis. *Proc Natl Acad Sci USA* 104(45):17582–17587.
21. Hasty J, *et al.* (2001) Designer gene networks: Towards fundamental cellular control. *Chaos* 11(1):207–220.
22. Warren PB, ten Wolde PR (2005) Chemical models of genetic toggle switches. *J Phys Chem B* 109(14):6812–6823.
23. Tian T, Burrage K (2006) Stochastic models for regulatory networks of the genetic toggle switch. *Proc Natl Acad Sci USA* 103(22):8372–8377.
24. Wernet MF, *et al.* (2006) Stochastic spineless expression creates the retinal mosaic for colour vision. *Nature* 440(7081):174–180.
25. Kepler TB, Elston TC (2001) Stochasticity in transcriptional regulation: origins, consequences, and mathematical representations. *Biophys J* 81(6):3116–3136.
26. Hasty J, *et al.* (2000) Noise-based switches and amplifiers for gene expression. *Proc Natl Acad Sci USA* 97(5):2075–2080.
27. Samoilov M, Plyasunov S, Arkin AP (2005) Stochastic amplification and signaling in enzymatic futile cycles through noise-induced bistability with oscillations. *Proc Natl Acad Sci USA* 102(7):2310–2315.
28. Horsthemke W, Lefever R (1984) *Noise-Induced Transitions: Theory and Applications in Physics, Chemistry, and Biology* (Springer, New York).
29. Vilar JM, *et al.* (2002) Mechanisms of noise-resistance in genetic oscillators. *Proc Natl Acad Sci USA* 99(9):5988–5992.
30. Biondi EG, *et al.* (2006) Regulation of the bacterial cell cycle by an integrated genetic circuit. *Nature* 444(7121):899–904.
31. Liu C, *et al.* (1997) Cellular construction of a circadian clock: period determination in the suprachiasmatic nuclei. *Cell* 91(6):855–860.
32. Mihalcescu I, Hsing W, Leibler S (2004) Resilient circadian oscillator revealed in individual cyanobacteria. *Nature* 430(6995):81–85.
33. Pomerening JR, Kim SY, Ferrell JE Jr (2005) Systems-level dissection of the cell-cycle oscillator: bypassing positive feedback produces damped oscillations. *Cell* 122(4):565–578.
34. Rust MJ, *et al.* (2007) Ordered phosphorylation governs oscillation of a three-protein circadian clock. *Science* 318(5851):809–812.
35. Yamaguchi S, *et al.* (2003) Synchronization of cellular clocks in the suprachiasmatic nucleus. *Science* 302(5649):1408–1412.
36. Keener J, Sneyd J (1998) *Mathematical Physiology* (Springer, New York).
37. Ozbudak EM, Becskei A, van Oudenaarden A (2005) A system of counteracting feedback loops regulates Cdc42p activity during spontaneous cell polarization. *Dev Cell* 9(4):565–571.
38. Muratov CB, Vanden-Eijnden E, Weinan E (2007) Noise can play an organizing role for the recurrent dynamics in excitable media. *Proc Natl Acad Sci USA* 104(3):702–707.
39. Klevecz RR (1976) Quantized generation time in mammalian cells as an expression of the cellular clock. *Proc Natl Acad Sci USA* 73(11):4012–4016.
40. Sveiczer A, Novak B, Mitchison JM (1996) The size control of fission yeast revisited. *J Cell Sci* 109(Pt 12):2947–2957.
41. Masui Y, Wang P (1998) Cell cycle transition in early embryonic development of Xenopus laevis. *Biol Cell* 90(8):537–548.
42. Sveiczer A, *et al.* (2000) Modeling the fission yeast cell cycle: quantized cycle times in wee1-cdc25Delta mutant cells. *Proc Natl Acad Sci USA* 97(14):7865–7870.
43. Steuer R (2004) Effects of stochasticity in models of the cell cycle: from quantized cycle times to noise-induced oscillations. *J Theor Biol* 228(3):293–301.
44. Koseska A, *et al.* (2007) Quantized cycling time in artificial gene networks induced by noise and intercell communication. *Phys Rev E Stat Nonlin Soft Matter Phys* 76(2 Pt 1):020901.
45. Gillespie DT (1977) Exact stochastic simulation of coupled chemical reactions. *J Phys Chem* 81:2340–2361.
46. Bashor CJ, *et al.* (2008) Using engineered scaffold interactions to reshape MAP kinase pathway signaling dynamics. *Science* 319(5869):1539–1543.
47. Strogatz SH (1994) *Nonlinear Dynamics and Chaos* (Addison-Wesley, Reading, MA).
48. Maheshri N, O'Shea EK (2007) Living with noisy genes: how cells function reliably with inherent variability in gene expression. *Annu Rev Biophys Biomol Struct* 36:413–434.
49. Raser JM, O'Shea EK (2005) Noise in gene expression: Origins, consequences, and control. *Science* 309(5743):2010–2013.
50. Dubnau D, Losick R (2006) Bistability in bacteria. *Mol Microbiol* 61(3):564–572.
51. Losick R, Desplan C (2008) Stochasticity and cell fate. *Science* 320(5872):65–68.
52. Arkin A, Ross J, McAdams HH (1998) Stochastic kinetic analysis of developmental pathway bifurcation in phage lambda-infected Escherichia coli cells. *Genetics* 149(4):1633–1648.
53. Weinberger LS, *et al.* (2005) Stochastic gene expression in a lentiviral positive-feedback loop: HIV-1 Tat fluctuations drive phenotypic diversity. *Cell* 122(2):169–182.
54. Chai Y, *et al.* (2008) Bistability and biofilm formation in Bacillus subtilis. *Mol Microbiol* 67(2):254–263.
55. Barkai N, Leibler S (2000) Circadian clocks limited by noise. *Nature* 403(6767):267–268.
56. Judd EM, Laub MT, McAdams HH (2000) Toggles and oscillators: New genetic circuit designs. *BioEssays* 22(6):507–509.
57. Lahav G, *et al.* (2004) Dynamics of the p53-Mdm2 feedback loop in individual cells. *Nat Genet* 36(2):147–150.
58. Laub MT, *et al.* (2000) Global analysis of the genetic network controlling a bacterial cell cycle. *Science* 290(5499):2144–2148.
59. Wang P, Hayden S, Masui Y (2000) Transition of the blastomere cell cycle from cell size-independent to size-dependent control at the midblastula stage in Xenopus laevis. *J Exp Zool* 287(2):128–144.